



ELSEVIER

Journal of Alloys and Compounds 321 (2001) 35–39

Journal of
ALLOYS
AND COMPOUNDS

www.elsevier.com/locate/jallcom

Magnetic properties of $\text{Nd}_{1-x}\text{Gd}_x\text{Mn}_2\text{Ge}_2$ compounds

S. Kervan^{a,b}, Y. Elerman^{a,*}, M. Acet^b^aPhysics Engineering, Science Faculty, Ankara University, 06100 Ankara, Turkey^bTiefemperaturphysik, Gerhard-Mercator Universität Duisburg, D-47048 Duisburg, Germany

Received 23 January 2001; accepted 13 February 2001

Abstract

The magnetic properties of polycrystalline $\text{Nd}_{1-x}\text{Gd}_x\text{Mn}_2\text{Ge}_2$ ($0 \leq x \leq 1$) compounds have been investigated by means of X-ray diffraction and measurements of the DC magnetization. All compounds crystallize in the ThCr_2Si_2 -type structure with the space group $I4/mmm$. Lattice parameters and the unit cell volume obey Vegard's law. The samples with $x \leq 0.6$ are ferromagnetic and have spin reorientation temperature. In the case of $0.7 \leq x < 1$, samples are ferrimagnetic with compensation point and reentrant ferrimagnetism is observed for $x=0.8$ and $x=0.85$. As a result, the magnetic phase diagram has been constructed. © 2001 Elsevier Science B.V. All rights reserved.

Keywords: Rare earth compounds; Transition metal compounds; Magnetically ordered materials; Phase transitions; Magnetic measurements

1. Introduction

The ternary intermetallic compounds of the formula RMn_2X_2 with R=rare-earth elements and X=Si or Ge have been extensively studied because of their interesting magnetic properties [1–3]. These compounds crystallize in the body-centered tetragonal ThCr_2Si_2 -type structure with the space group $I4/mmm$, in which R, Mn and X atoms occupy $2a(0,0,0)$, $2d(0,1/2,1/4)$ and $4e(0,0,z)$ sites, respectively [4]. This structure can be described as a stacking of atomic layers along the c -axis direction with the sequence Mn–X–R–X–Mn. The magnetic properties of these compounds are very sensitive to the intralayer Mn–Mn spacing $R_{\text{Mn–Mn}}^a$. It was found that ferromagnetic phase is observed when $R_{\text{Mn–Mn}}^a$ is larger than a critical value of 2.85 Å whereas antiferromagnetic phase is stable when $R_{\text{Mn–Mn}}^a$ is smaller than 2.85 Å [5].

Mössbauer spectroscopy [6], neutron scattering [7,8], magnetization on single crystal [9] and polycrystal [2,7,10] studies show four phase transitions in NdMn_2Ge_2 compound. According to above references, various values of transition temperatures have been found for $T_C(\text{Nd})$ (21, 40, 100 K), $T_{\text{SR}}(\text{Mn})$ (210, 215, 250 K), $T_C(\text{Mn})$ (330, 334, 336, 339 K) and $T_N(\text{Mn})$ (415, 430 K). Below the

spin reorientation temperature (T_{SR}), the Mn sublattice has conical ferromagnetic structure down to low temperatures. Above T_{SR} , canted ferromagnetic structure occurs up to the $T_C(\text{Mn})$. Antiferromagnetic Mn layers along a are stabilized between $T_C(\text{Mn})$ and $T_N(\text{Mn})$, and the compound is paramagnet for $T > T_N(\text{Mn})$. The Nd sublattice acquires a ferromagnetic arrangement along the a -axis and is ferromagnetically coupled to the Mn layers below $T_C(\text{Nd})$.

GdMn_2Ge_2 is a collinear ferrimagnet for $T < 95$ K and transforms to an antiferromagnet with a first order transition above this temperature. In the ferrimagnetic temperature range, along the c -axis, the moment on Gd is aligned antiparallel to the Mn moment. Above 95 K, the Gd moments are disaligned and the Mn sublattice acquires a collinear antiferromagnetic structure that persists up to 365 K. Above this temperature, GdMn_2Ge_2 is a weak ferromagnet in a narrow temperature range and becomes paramagnetic above about 480 K [11–13].

This study reports the influence of substitution of Gd for Nd on crystal structure and magnetic properties of $\text{Nd}_{1-x}\text{Gd}_x\text{Mn}_2\text{Ge}_2$.

2. Experimental

$\text{Nd}_{1-x}\text{Gd}_x\text{Mn}_2\text{Ge}_2$ compounds with $x=0.0, 0.2, 0.4, 0.5, 0.6, 0.7, 0.75, 0.8, 0.85$ and 1.0 were prepared by induction melting constituent elements under Ar atmosphere in a

*Corresponding author. Tel.: +90-312-212-6720; fax: +90-312-223-2395.

E-mail address: elerman@science.ankara.edu.tr (Y. Elerman).

water-cooled copper boat. The purity of the elements were 99.9% for Nd and Gd, 99.98% for Mn and 99.9999% for Ge. Adding the 2% excess Mn over the stoichiometric amount compensated the mass loss of Mn during the melting. In order to achieve good homogeneity, the polycrystalline ingots were turned over and remelted several times.

X-ray diffraction studies were carried out by using Rigaku D-Max 2200 diffractometer equipped with $\text{CuK}\alpha$ radiation. The magnetic properties of $\text{Nd}_{1-x}\text{Gd}_x\text{Mn}_2\text{Ge}_2$ compounds were studied by means of a SQUID magnetometer (Quantum Design) in the temperature range 5–350 K in magnetic fields up to 5 T. Magnetization measurements above room temperature were done using a vibrating sample magnetometer.

3. Results and discussion

The X-ray patterns confirm that all compounds are single phase and crystallize in the ThCr_2Si_2 -type structure. The refined lattice parameters a and c , unit cell volume V and intralayer Mn–Mn distance $R_{\text{Mn–Mn}}^a$ are shown in Fig. 1 and the values are listed in Table 1. The linear decrease of the lattice constants a and c , and the unit cell volume V , which may be associated with the smaller atomic radius of Gd compared with Nd, shows that these parameters obey Vegard's law.

The thermal variation of the magnetization of the $\text{Nd}_{1-x}\text{Gd}_x\text{Mn}_2\text{Ge}_2$ compounds in the temperature range 5–350 K in applied field of 400 Oe is presented in Fig. 2. The obtained transition temperatures (Table 2) for the samples with $x=0$ and $x=1$ are in good agreement with the values reported in the literature. At low temperatures, GdMn_2Ge_2 is ferrimagnetic due to negative Gd–Mn exchange interaction stabilized at low volume [13]. This compound shows antiferromagnetic behavior between the first order phase transition temperature (95 K) from ferrimagnetism to antiferromagnetism and the Néel temperature of 364 K. Above the Néel temperature, there is a small spontaneous magnetization indicating that GdMn_2Ge_2 is a weak ferromagnet with $T_{\text{C}2}$ of 460 K. The spin reorientation observed in NdMn_2Ge_2 , which leads to phase transition from a conical ferromagnetic structure to a canted ferromagnetic structure, is depressed by the substitution of Gd for Nd and disappears for the compounds with $x>0.6$. The spin reorientation temperature (T_{SR}) was defined by the cusp maximum of $M(T)$ curves. The width of cusp broadens with increasing x . Below T_{SR} , another transition is seen at about 20 K (T_{R}), which is attributed to the ordering of R sublattice. Below T_{R} , magnetization increases with decreasing temperature for $x=0$ and $x=0.2$, and decreases for $x=0.4$. This may be explained by assuming that in these compounds the rare earth sublattice couples either ferromagnetic or antiferromagnetically to the Mn sublattice in the case of light (Nd) or heavy rare

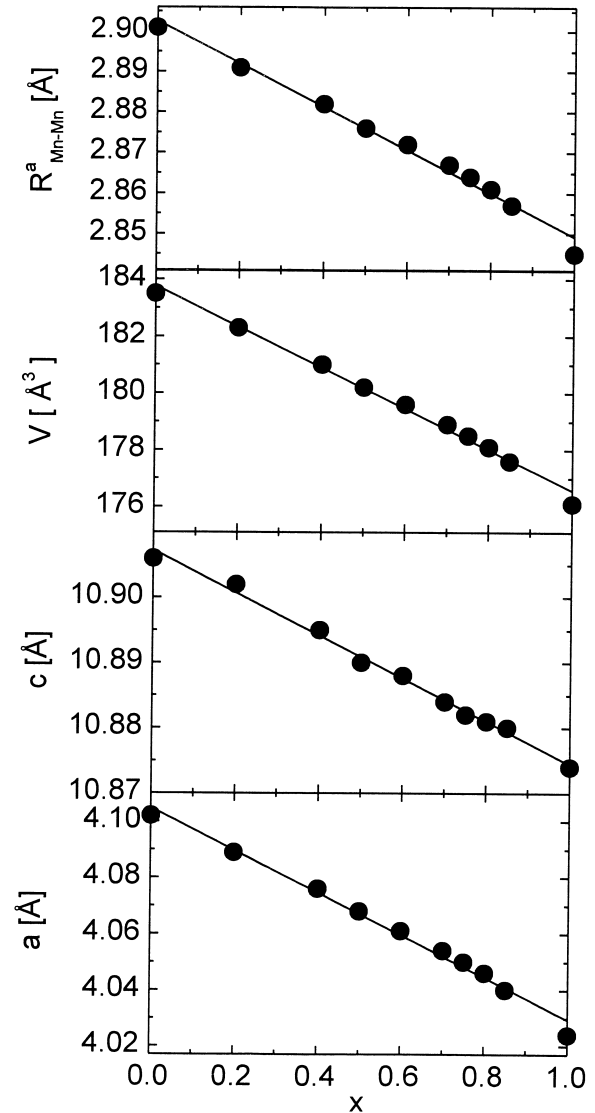


Fig. 1. Variation of the lattice constants a and c , unit cell volume V and the intralayer nearest Mn–Mn distance $R_{\text{Mn–Mn}}^a$ with Gd concentration x at room temperature for the $\text{Nd}_{1-x}\text{Gd}_x\text{Mn}_2\text{Ge}_2$ compounds.

Table 1

The lattice constants a and c , the unit cell volume V , and the intralayer nearest Mn–Mn distance $R_{\text{Mn–Mn}}^a$ for the $\text{Nd}_{1-x}\text{Gd}_x\text{Mn}_2\text{Ge}_2$ compounds

x	a (Å)	c (Å)	V (Å ³)	$R_{\text{Mn–Mn}}^a$ (Å)
0.0	4.102	10.906	183.5	2.901
0.2	4.089	10.902	182.3	2.891
0.4	4.076	10.895	181.0	2.882
0.5	4.068	10.890	180.2	2.876
0.6	4.061	10.888	179.6	2.872
0.7	4.054	10.884	178.9	2.867
0.75	4.050	10.882	178.5	2.864
0.8	4.046	10.881	178.1	2.861
0.85	4.040	10.880	177.6	2.857
1.0	4.024	10.874	176.1	2.845

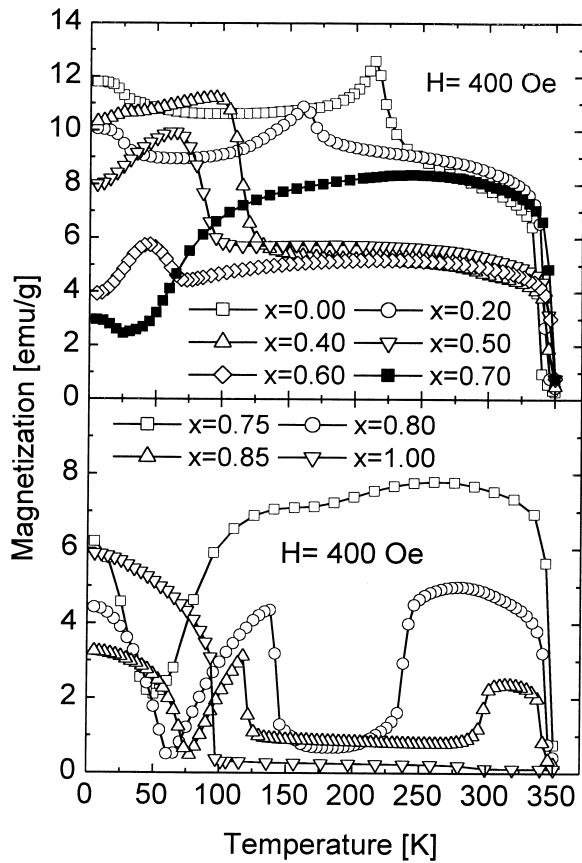


Fig. 2. Temperature dependence of the magnetization in the temperature range 5–350 K for $\text{Nd}_{1-x}\text{Gd}_x\text{Mn}_2\text{Ge}_2$ compounds in a magnetic field of 400 Oe.

earth (Gd), respectively. If we take into account free Nd^{+3} ($3.3 \mu_B$) and Gd^{+3} ($7.0 \mu_B$) ions, the Nd magnetic moment becomes dominant for $x=0.2$ and the Gd magnetic moment becomes dominant for $x=0.4$ in the R sublattice, and thus the magnetization increases for $x=0.2$ and decreases for $x=0.4$ below T_R . The compensation temperature is seen for the samples with $0.7 \leq x < 1$. Bearing in mind that the magnetic moment of the R sublattice decreases more rapidly with increasing temperature than the magnetic moment of the Mn sublattice and taking into account that the total magnetic moment of R sublattice increases with

increasing Gd content for $x \geq 0.7$, the Mn sublattice moment can cancel the R sublattice moment at higher temperatures. Therefore, the compensation temperature increases monotonously.

Reentrant ferrimagnetism is observed for the samples with $x=0.8$ and $x=0.85$. For these samples, the $R_{\text{Mn-Mn}}^a$ values at room temperature are very close to the critical value. The lattice contraction due to cooling causes a transition from the ferrimagnetic phase to the antiferromagnetic phase at T_2 . This antiferromagnetic phase is stable down to T_1 and then again a transition takes place because of the negative R–Mn exchange interaction. A trace of antiferromagnetic phase is seen for $x=0.75$. The variation of T_1 and T_2 in opposite direction with increasing x induces a broadening of the width of the antiferromagnetic phase region, which can be correlated to the decrease of the intralayer Mn–Mn distance $R_{\text{Mn-Mn}}^a$. The intralayer Mn–Mn distance $R_{\text{Mn-Mn}}^a$ in these samples decreases linearly with increasing x . The decrease of the $R_{\text{Mn-Mn}}^a$ weakens the ferromagnetic coupling, yielding broadening of antiferromagnetic phase region. As a result, the stability of antiferromagnetic phase increases with increasing x and the ferrimagnetic phase between T_2 and T_{C1} disappears for $x=1$.

Fig. 3 exhibits the temperature dependence of the magnetization above room temperature in an applied field of 400 Oe. The saturation behavior with a small magnetization value indicates the presence of a weak ferromagnetic phase in the temperature range $T_{C1} < T < T_{C2}$. This may be due to the unstable antiferromagnetic Mn–Mn coupling [11].

For $x=0.8$ and $x=0.85$, Fig. 4 shows the magnetization as a function of applied field at various temperatures. A field induced metamagnetic transition from antiferromagnetism to ferrimagnetism occurs at about 1 T. A multi-step increase of the magnetization takes place for $x=0.8$ at $T=146$ K, which may be attributed to a step-like growth of ferrimagnetic domains in the layered antiferromagnet.

Fig. 5 shows the magnetization of the $\text{Nd}_{1-x}\text{Gd}_x\text{Mn}_2\text{Ge}_2$ compounds as a function of applied field at 5 K up to the 50 kOe. The values of saturation magnetization as a function of Gd concentration are drawn in Fig. 6 and are

Table 2

The magnetic transition temperatures T_R , T_{comp} , T_{SR} , T_1 , T_2 , T_{C1} , T_{C2} , T_N and the saturation magnetization μ_S at 5 K for the $\text{Nd}_{1-x}\text{Gd}_x\text{Mn}_2\text{Ge}_2$ compounds

x	T_R (K)	T_{SR} (K)	T_{comp} (K)	T_1 (K)	T_2 (K)	T_{C1} (K)	T_{C2} (K)	T_N (K)	μ_S [$\mu_B/\text{f.u.}$]
0.0	23	214				336		430	4.70
0.2	25	160				342			3.16
0.4	18	90				345			2.06
0.5		60				346	442		1.28
0.6		45				346	445		0.54
0.7			25			346	448		0.53
0.75			50			345	453		0.75
0.8			62	141	238	342	456		0.76
0.85			77	121	298	342	458		1.15
1.0						95	460	364	1.99

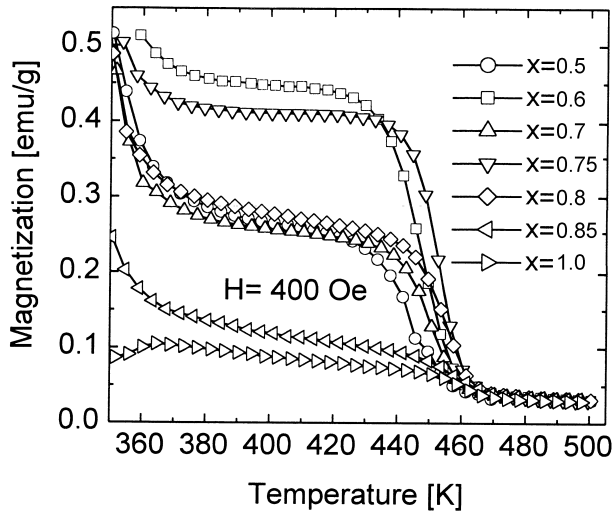


Fig. 3. Temperature dependence of the magnetization above room temperature for $Nd_{1-x}Gd_xMn_2Ge_2$ compounds in a magnetic field of 400 Oe.

also listed in Table 2. The saturation magnetization decreases with increasing x at 5 K up to $x=0.7$, and then increases again.

The magnetic phase diagram for the $Nd_{1-x}Gd_xMn_2Ge_2$, summarizing the results, is presented in Fig. 7. The

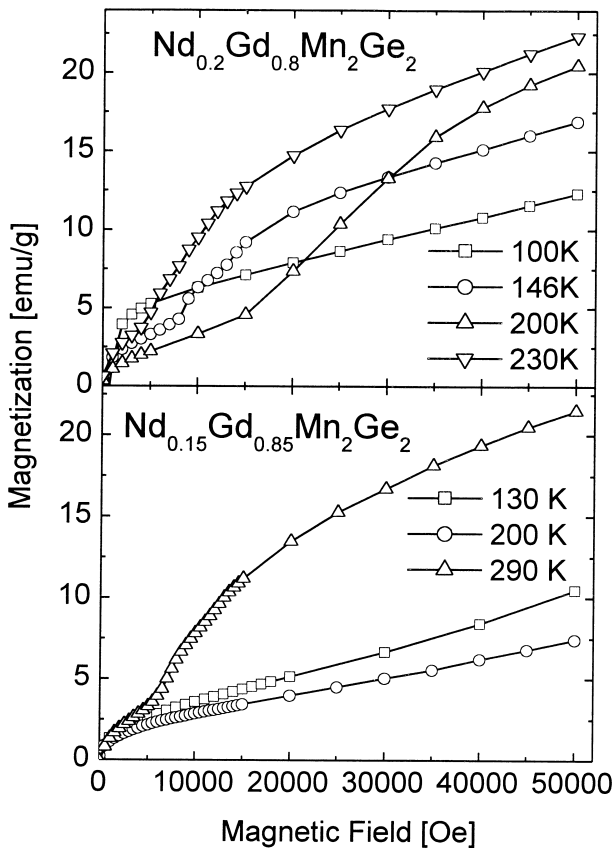


Fig. 4. Magnetization as a function of applied field for $x=0.8$ and $x=0.85$ at various temperatures.

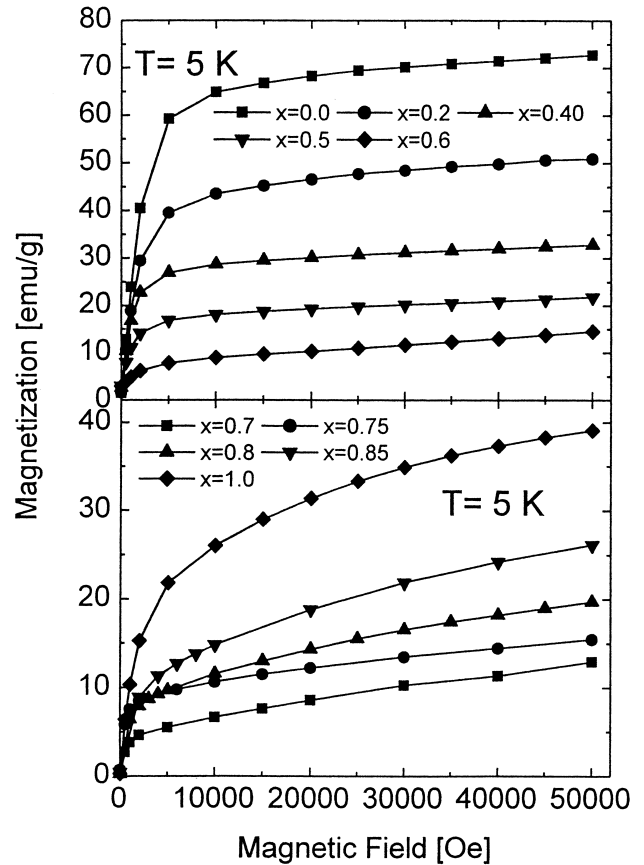


Fig. 5. Magnetization of $Nd_{1-x}Gd_xMn_2Ge_2$ compounds as a function of applied field at 5 K up to the 5 T.

transition temperatures are also listed in Table 2. The spin reorientation temperature decreases linearly with increasing x from 214 K at $x=0$ to 45 K at $x=0.6$. The compensation temperature increases monotonously with increasing x . In the light of results in the literature [14], we completed $T_1(x)$ and $T_2(x)$ in the magnetic phase diagram. The $T_N(Mn)$ value for $NdMn_2Ge_2$ was taken from the literature and connected to T_{C2} to define the AF phase region.

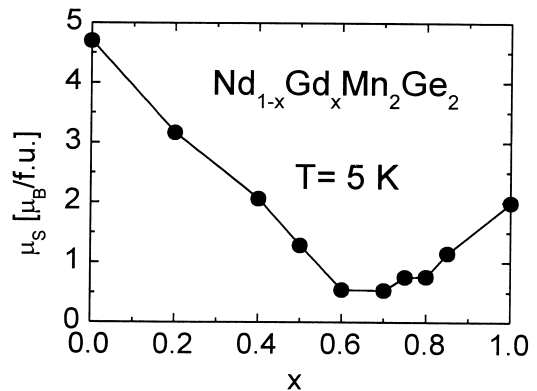


Fig. 6. Saturation magnetization as a function of Gd concentration x of $Nd_{1-x}Gd_xMn_2Ge_2$ compounds.

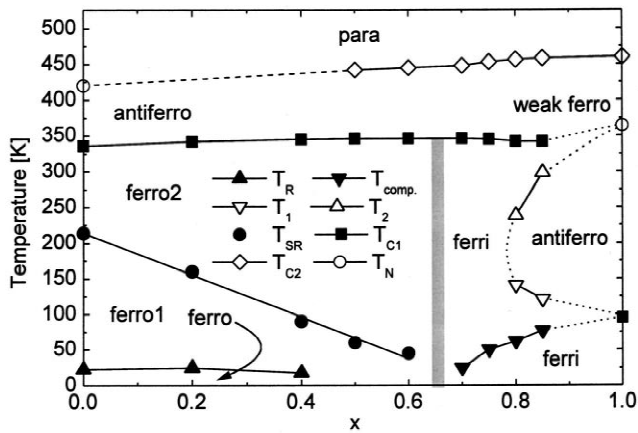


Fig. 7. Magnetic phase diagram of $\text{Nd}_{1-x}\text{Gd}_x\text{Mn}_2\text{Ge}_2$ compounds.

4. Conclusions

All the $\text{Nd}_{1-x}\text{Gd}_x\text{Mn}_2\text{Ge}_2$ compounds crystallize in the ThCr_2Si_2 -type structure. Substitution of Gd for Nd causes linear increases in the lattice constants and unit cell volume from $a=4.102 \text{ \AA}$, $c=10.906 \text{ \AA}$, and $V=183.5 \text{ \AA}^3$ for $x=0$ to $a=4.024 \text{ \AA}$, $c=10.874 \text{ \AA}$, and $V=176.1 \text{ \AA}^3$ for $x=1$. Ferromagnetism observed in NdMn_2Ge_2 transforms to ferrimagnetism with the substitution of Gd (heavy rare earth) for Nd (light rare earth). The saturation magnetization at 5 K decreases up to $x=0.7$ and then increases again. Reentrant ferrimagnetism is observed for $x=0.8$ and $x=0.85$. Consequently, the $x-T$ magnetic phase diagram has been established from the derived transitions temperatures.

Acknowledgements

One of the authors (S.K.) would like to thank to Mrs Ö. Çakir for helping during the X-ray measurements. This

work was supported by Research Funds of the University of Ankara under grant number 98-05-05-01 and The Scientific and Technical Research Council of Turkey (TÜBİTAK-BAYG).

References

- [1] A. Szytula, J. Leciejewicz, in: K.A. Gschneidner, Jr., L. Eyring (Eds.), Handbook on the Physics and Chemistry of Rare Earths, Vol. 12, 1989, p. 133.
- [2] K.S.V.L. Narasimhan, V.U.S. Rao, R.L. Bergner, W.E. Wallace, J. Appl. Phys. 46 (1975) 4957.
- [3] A. Szytula, J. Alloys Comp. 178 (1992) 1.
- [4] Z. Ban, M. Sikirica, Acta Cryst. 18 (1965) 594.
- [5] H. Fujii, T. Okamoto, T. Shigeoka, N. Iawata, Solid State Commun. 53 (1985) 715.
- [6] I. Nowik, Y. Levi, I. Felner, E.R. Bauminger, J. Magn. Magn. Mater. 147 (1995) 373.
- [7] R. Welter, G. Venturini, E. Ressouche, B. Malaman, J. Alloys Comp. 218 (1995) 204.
- [8] L. Morellon, P.A. Algarabel, M.R. Ibarra, Phys. Rev. B 55 (1997) 12363.
- [9] T. Shigeoka, N. Iwata, H. Fuji, J. Magn. Magn. Mater. 76and77 (1988) 189.
- [10] Y.-G. Wang, F. Yang, C. Chen, N. Tang, Q. Wang, Phys. Stat. Sol.(a) 162 (1997) 723.
- [11] T. Shigeoka, H. Fujii, H. Fujiware, K. Yagosaki, T. Okamoto, J. Magn. Magn. Mater. 31–34 (1983) 209.
- [12] H. Kobayashi, H. Onodera, H. Yamamoto, J. Magn. Magn. Mater. 79 (1989) 76.
- [13] N. Iwata, K. Hattori, T. Shigeoka, J. Magn. Magn. Mater. 53 (1986) 318.
- [14] A. Sokolov, H. Wada, M. Shiga, T. Goto, Solid State Commun. 105 (1998) 289.